SMiRT-12 / K. Kussmaul (Editor)

K23/1

RESPONSE OF SEISMIC ISOLATED FACILITIES: A PARAMETRIC STUDY OF THE ALMR

F.F. Tajirian[1] and M.R. Patel[2]

[1]Bechtel National Inc., San Francisco, CA, USA
[2]General Electric Company, San Jose, CA, USA

ABSTRACT

The seismic response of the isolated Advanced Liquid Metal Reactor (ALMR) is investigated using three-dimensional linear and nonlinear models. Dynamic analyses are performed for earthquake levels ranging from one-fourth the ALMR design safe shutdown earthquake (SSE, 0.075g) to more than six times the SSE (2.0 g input). The results show that the horizontal seismic response of the ALMR is insensitive to variations in modeling techniques, type of analysis (linear or nonlinear), soil flexibility, and the characteristics of the design earthquake. The vertical response is primarily influenced by the soil flexibility and vertical dynamic properties of the isolated structures and components. The effect of stiffening that occurs in elastomeric based isolators at high shear strains on system response is examined. When the increased stiffness is accounted for in the analysis, the computed displacements for extreme events are reduced by up to thirty percent.

1 INTRODUCTION

The ALMR program sponsored by the U.S. Department of Energy (DOE) uses seismic isolation to simplify design, to enhance safety margins, and to support the development of a standardized design for the majority of the available U.S. reactor sites. The ALMR [Quinn et al. 1992], employs compact reactor modules sized to enable factory fabrication, and ease of shipment to a wide range of sites. The isolated structural configuration investigated in this paper consists of a stiff rectangular steel-concrete box structure 52 ft × 91 ft (15.9 m × 27.7 m). It supports the reactor vessel, the containment dome and the reactor vessel auxiliary cooling system stacks. The reactor vessel has a 20 ft (6.1 m) diameter and a height of 62 ft (18.9 m) and is supported from the top. The relatively small diameter of the vessel provides sufficient intrinsic resistance in the vertical direction to minimize amplifications in the vertical ground motions making vertical isolation unnecessary. The isolated structure weighs 13,000 kips (5800 tons) and is supported on 25 seismic isolation bearings. The isolators consist of steel-laminated elastomeric bearings using a high damping compound. The horizontal isolation frequency is 0.75 Hz, and the vertical frequency is greater than 20 Hz. Other ALMR plant configurations are presently under study including a design which supports the steam generator on a larger common isolated platform using 48 bearings.

A comprehensive seismic analysis plan has been developed to confirm the adequacy of the design and to support regulatory licensing activities. In this paper, various factors that may affect the seismic response are investigated. These include nonlinear response of the isolators, effect of the isolators on vertical seismic response, variability in the input earthquake mechanism including the size of the earthquake, and soil-structure interaction effects. The results of linear and nonlinear seismic analyses are summarized.

2 SEISMIC CRITERIA

The ALMR is designed to accommodate the seismic conditions expected at a wide range of sites, from deep soil sites with a minimum shear wave velocity of 1000 fps (305 m/s), to stiff rock sites. The present licensing seismic design basis is a safe shutdown earthquake (SSE) with a maximum horizontal and vertical acceleration (PGA) of 0.3g. The design earthquake is consistent with the U.S. NRC Regulatory Guide 1.60 spectra. However, a PGA of 0.5g is being used to design the nuclear island. Figure 1 shows a comparison of the RG 1.60 design spectrum with the tentative Japanese design spectrum developed specifically for seismically isolated FBRs [Ishida et al. 1989]. It can be seen that for frequencies that are important to the response of isolated structures (0.5 to 1.0 Hz), the two curves are alike. Figure 1 also shows response spectra developed by the Electric Power Research Institute [EPRI 1989] for Central or Eastern USA. Spectra for two siting conditions. The EPRI spectra have lower long period components than the RG 1.60 spectrum which was originally developed from earthquakes recorded in the Western United States. For example at 1 Hz the RG 1.60 spectrum normalized to 1.0g PGA has a spectral acceleration of 1.5g. The equivalent EPRI spectral accelerations are 1g for the soil site and 0.5g for the rock site. Thus, for a given peak ground acceleration, designs of isolated structures based on RG 1.60 spectra will have higher margins at sites where the EPRI spectra are applicable.

3 LINEAR SEISMIC ANALYSIS

A three-dimensional model was developed to represent the isolated ALMR. The seismic platform and reactor model are shown in Figure 2. Input time histories that envelop the RG 1.60 spectra were scaled to 0.3g for the SSE and to 0.1g to represent small earthquakes. Soil-structure interaction (SSI) effects were modeled as frequency independent springs. Composite modal damping was used to include soil damping. Two sites were investigated; a rigid site, and a soft site with a shear wave velocity of 1000 ft/s (305 m/s). The seismic isolators used for the ALMR have nonlinear characteristics. At the low strain levels expected during small eathquakes, their horizontal stiffness is higher than at strains resulting from the design earthquake. The 25 seismic isolators were modeled with beam elements with equivalant linear strain compatible stiffness properties. For the SSE case the isolator horizontal stiffness was equivalent to a frequency of 0.75 Hz. For the smaller earthquake, this stiffness was increased by a factor of 2.5, increasing the isolation frequency to 1.16 Hz. This factor was based on half-scale bearing tests [Tajirian et al. 1992].

For the SSE level input the maximum horizontal accelerations are reduced by the isolators from 0.3g to 0.26g in both horizontal directions. Furthermore, the isolated structure moves as a rigid body and there is very little amplification in horizontal accelerations. Figure 3 compares the response spectra on the lower mat below the isolators with the spectra at the reactor vessel supports. The results for the two horizontal directions and two site conditions are shown. The isolators are very effective in reducing spectral accelerations above 1.2 Hz. The figure shows that the isolated response is not sensitive to variations in the input motion or soil stiffness even though the spectra below the isolators differ significantly above 5Hz. In fact unlike conventional structures, the response of isolated structures is governed by input response in the range between 1 and 3 seconds (0.3 Hz to 1 Hz) and is unaffected by changes that affect frequencies greater than 2 Hz. SSI effects seldom modify response within the applicable low frequency range. This is a major advantage of using seismic isolation over conventional plant design, where significant effort is consumed during the design phase to account for uncertainties in structural response due to changes in input time history and SSI effects. Another advantage is that high frequency motions which control the response of conventional structures are stochastic and can reach very large values (>2g) in extreme cases. Conversely, low frequency components that affect isolated structures are deterministic and can be predicted reasonably well if the overall seismic source parameter values are known [Spudich and Archuleta 1987; Tajirian and Abrahamson 1991; Somerville and Graves 1993]. Furthermore, displacements during an extreme event are bounded by the physical characteristics of the seismic source and thus are numerically more stable.

The vertical spectra below and above the isolators are compared in Figure 4a and 4b. It can be seen that the amplification across the isolators is small for both sites. The peak at about 9 Hz for the soil case corresponds to the vertical foundation-soil frequency and is independent of the vertical stiffness of the isolators. A more detailed SSI analysis is required to accurately quantify the vertical amplifications in foundation response resulting from the flexibility of the soil. It is expected that more accurate modeling of embedment will reduce the amount of amplification calculated in this study. For the rock case the amplifications at frequencies greater than 10 Hz are partly attributed to the vertical flexibility of the isolated concrete platform. These peaks are not present in the soil case because of the beneficial damping effects present in the softer sites.

To study the effect of a small earthquake, the input time history used above was scaled to a maximum acceleration of 0.1g. For this case the maximum horizontal acceleration on the seismic platform was amplified to 0.13g. Such amplifications have also been observed in the response of isolated buildings during small earthquakes [Kelly et al. 1992; Clark et al. 1993]. This phenomenon is well understood and as shown in this study is predictable even with the use of simple equivalent linear models. The horizontal spectra above the isolators are compared with the equivalent spectra for the SSE case widened by plus or minus 15 percent in Figure 5. As shown the smaller earthquake may cause spectral accelerations at about 1.2 Hz to be higher than the SSE widened spectra. The impact of this observation should be considered when evaluating the response of equipment and other components with frequencies less than 2 Hz.

4 NONLINEAR SEISMIC ANALYSIS

The same ALMR configuration analyzed above was also analyzed with a nonlinear representation of the isolators. The objective of this analysis was to evaluate the effects of increases in bearing stiffness at high strains and to compare the results with the equivalent linear analysis. The seismic platform was modeled as an assemblage of rigid beams. The isolators were modeled as individual springs to properly model rocking and torsional effects. In the axial direction, the springs were linear. In the two lateral directions, the springs were nonlinear, and had three stiffness segments as shown in Figure 6. Damping of the isolators was provided as hysteretic damping in the springs. Additional effective damping of about 1 percent was introduced as Rayleigh damping. A single lumped mass spring model was used to represent the reactor system. The site was assumed rigid.

A parametric study was performed to compute the response of the platform. The parameters that were modified included the input time history, the peak acceleration, the ratio of the third stiffness, K_3, to the mid stiffness, K_2, and the horizontal deflection δ_s at which the bearing stiffness increases (see Figure 7).

The analyses were performed for earthquake levels ranging from one-fourth the SSE (0.075g input) to more than six times the SSE (2.0g input). The isolator stiffnesses were adjusted to make them compatible with the input acceleration level. The RG 1.60 input time histories used in the linear analyses were scaled to 0.075g, 0.15g, 0.75g, 1.0g, and 2.0g. For the extreme case, an additional set of time histories was generated through numerical analysis for a hypothetical site in California. It was developed assuming a moment magnitude 8.5 on the San Andreas fault [Tajirian and Abrahamson 1991]. This condition represented an upper bound event for California. The resulting time histories had a maximum horizontal acceleration of 2.0g and a maximum vertical acceleration of 1.2g.

The combined displacements computed for the low level inputs were 1 in. (2.54 cm) for 0.075g and 2 in. (5.08 cm) for 0.15g. It should be noted that the equivalent displacements computed using the equivalent linear approach described in the previous section was 1.29 in. (3.28 cm) for 0.1g input. This compares well with the nonlinear results (1.33 in. obtained by interpolating the nonlinear results). The displacement computed using the linear model compatible with the 0.3g input was 6.23 in., or 2.08 in. (5.28 cm) for 0.1g input. It can be thus concluded that the equivalent linear model used for the small earthquake is more appropriate. For 0.75g and 1.0g inputs the nonlinear solutions give 16.6 in. (42.2 cm) and 21.6 in. (54.9 cm) respectively. Scaling the linear results (0.3g model) to these levels would give 15.6 in. (39.6 cm) and 20.8 in. (52.8 cm) indicating that the model is adequate in the range of input from 0.3g to 1.0g,

which is within the bearing stiffness range that is constant. This finding has also been confirmed by other investigators [Kitamura et al. 1992; Sanò et al. 1992].

To examine the effect of bearing stiffening at high shear strains on limiting extreme displacements, the results for the four different K_3/K_2 ratios defined in Figure 7 are plotted in Figure 8. The input for all for cases is the RG compatible scaled to 2.0g. It can be seen that with no bearing stiffening, the maximum combined displacement is 62.5 in. (159 cm). The displacement decreases as the stiffness ratio increases. For K_3/K_2 of 10 the displacement is reduced to 41 in. (104 cm). Although the increase in stiffness is beneficial in limiting displacements it results in an increase in the forces in the isolated structure. The effect of this on component margins has to be assessed. Another parameter which was varied was the lateral displacement δ_s beyond which the bearing was assumed to stiffen. The K_3/K_2 was held constant at a value of 4.2. The analysis was performed with the extreme input and three value of δ_s, 1.5 ft. (45.7 cm), 2.0 ft. (61 cm), and 2.5 ft. (76 cm). The same analysis was performed with the RG 1.60 input scaled to 2.0g with δ_s of 2.0 and 2.5 ft. The maximum combined displacements for the various cases are compared in Figure 9. It can be concluded from this figure that the displacements are reduced if a bearing design with a shorter rubber stack is used where the stiffness starts increasing at a lower displacement. It can also be concluded from this figure that the two different time histories used result in similar responses. The effects of vertical nonlinearities in the bearings and any coupling with horizontal response will be investigated in future studies.

REFERENCES

Electric Power Research Institute (1989), *Probabilistic Seismic Hazard Evaluation at Nuclear Power Plant Sites in the Central and Eastern United States: Resolution of the Charleston Earthquake Issue*, NP-6395-D, April.

Clark, P. W., Whittaker, A. S., Aiken, I. D., and Egan, J. A. (1993) "Performance Considerations for Isolation Systems in Regions of High Seismicity," *Seminar on Seismic Isolation, Passive Energy Dissipation, and Active Control,* ATC-17-1, Vol. 1.

Ishida, K., et al. (1989), "Tentative Design Response Spectrum for Seismically Isolated FBR," *Transactions of 10th SMiRT Conference*, Vol. K2, Anaheim, California, August.

Kelly, J. M., Aiken, I. D., and Clark, P. W. (1992), "Response of Base-Isolated Structures in Recent Earthquakes," *10th Structures Congress*, ASCE, April.

Kitamura, S., Morishita, M., and Iwata, K. (1992), "3-D Seismic Response of a Base-Isolated Fast Reactor," *IAEA Specialists' Meeting Seismic Isolation Technology*, San Jose, CA.

Quinn, J. E., Boardman, C. E., Thompson, M. L., and Snyder, C. R. (1992), "US ALMR, A Multi-Mission Advanced Reactor Concept for the Next Century," *Int. Conference on Design and Safety of Advanced Nuclear Power Plants*, Tokyo.

Sanò, T., Di Pasquale, G., and Vicaturo, E. (1992), "Linear Analysis for Base-Isolated Structures," *IAEA Specialists' Meeting Seismic Isolation Technology*, San Jose, CA, March.

Somerville, P., and Graves, R. (1993), "Conditions that Give Rise to Unusually Large Long Period Ground Motions," *Seminar on Seismic Isolation, Passive Energy Dissipation, and Active Control,* ATC-17-1, Vol. 1.

Spudich, P. and Archuleta (1987), *Complete Strong Motion Synthetics in Seismic Strong Motion Synthetics*, B. Bolt, ed., Academic Press, pp 153-204.

Tajirian, F. F., and Abrahamson, N. A. (1991), "Response of Seismic Isolated Structures During Extreme Events," *Transactions of 11th SMiRT Conference*, Vol. K2, Tokyo, August.

Tajirian, F. F., Gluekler, E. L., Chen, P., and Kelly, J. M. (1992), "Qualification of High Damping Seismic Isolation Bearings for the ALMR," *IAEA Specialists' Meeting Seismic Isolation Technology*, San Jose, CA, March.

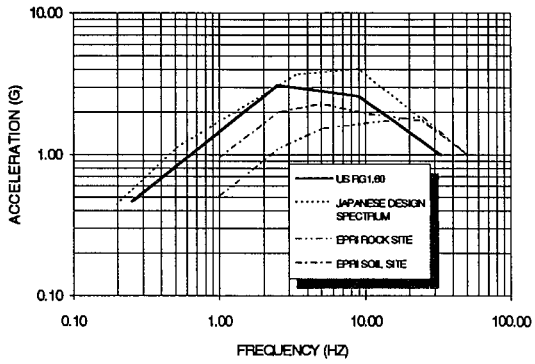

Fig. 1 Comparison of Horizontal Design Spectra 5 Percent Damping.

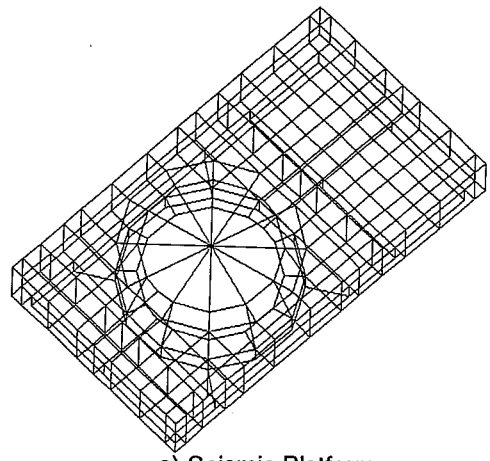

a) Seismic Platform

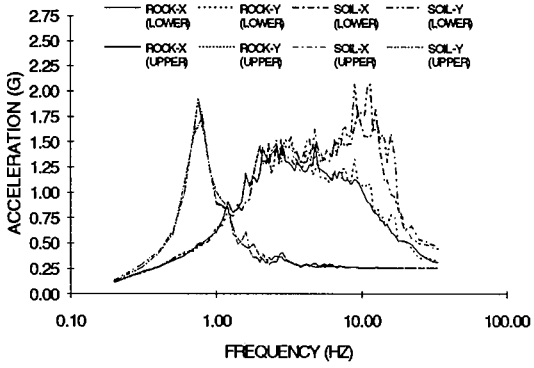

Fig. 3 Comparison of Horizontal Spectra, Lower Mat and R/V Support, 2 Percent Damping

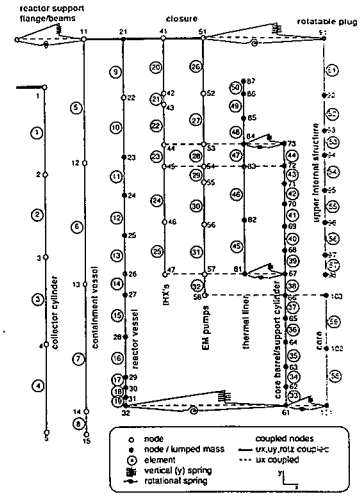

b) Reactor Model

Fig. 2 ALMR Seismic Analysis Model

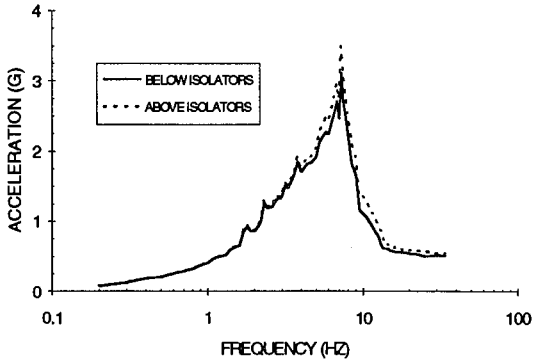

a) Soil Case

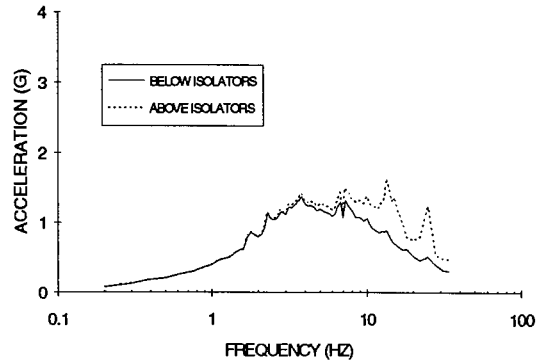

b) Rock Case

Fig. 4 Comparison of Vertical Spectra, Lower Mat and Isolated Platform, 2 Percent Damping

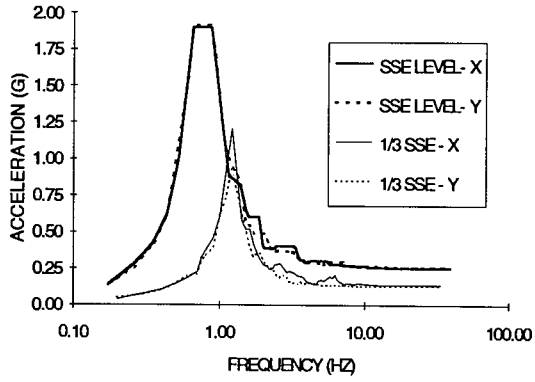

Fig. 5 Comparison of Horizontal Spectra on Isolated Platform for SSE and 1/3 SSE

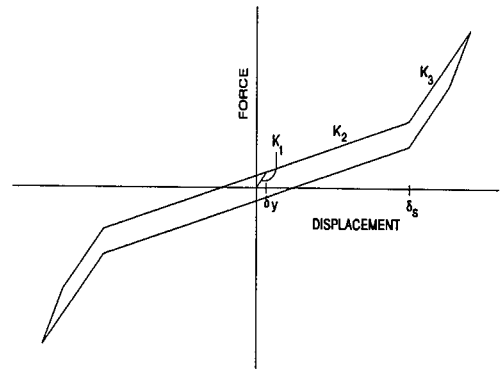

Fig. 6 Isolation Bearing Nonlinear Model

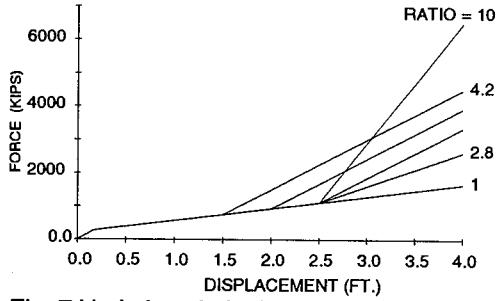

Fig. 7 Variations in Isolation Bearing Spring Properties

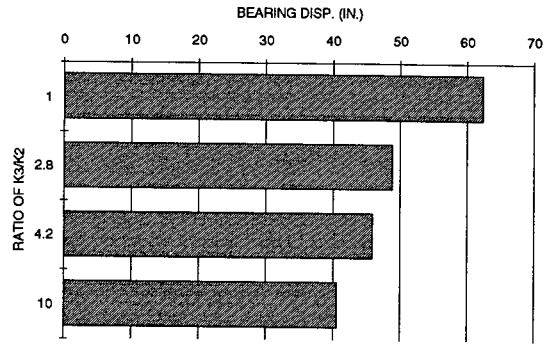

Fig. 8 Effect of Isolator Stiffening on Maximum Displacement, 2.0g Input

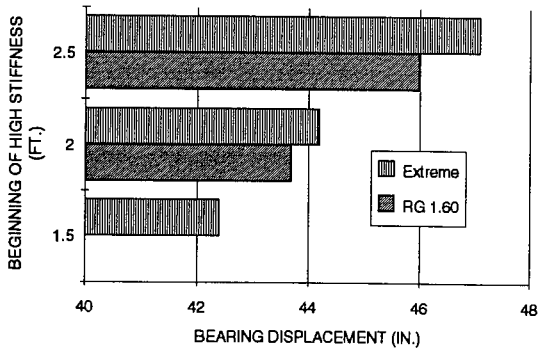

Fig. 9 Effect of Varying Dispacement δ_S on Total Bearing Displacement, 2.0g Input